MAGNETIC RESONANCE IN MEDICINE **14,** 68–78 (1990)

Oxygenation-Sensitive Contrast in Magnetic Resonance Image of Rodent Brain at High Magnetic Fields

SEIJI OGAWA, TSO-MING LEE, ASHA S. NAYAK,* AND PAUL GLYNN

AT&T Bell Laboratories, Murray Hill, New Jersey 07974

Received November 30, 1988; accepted June 20, 1989

At high magnetic fields (7 and 8.4 T), water proton magnetic resonance images of brains of live mice and rats under pentobarbital anesthetization have been measured by a gradient echo pulse sequence with a spatial resolution of 65 × 65-μm pixel size and 700-μm slice thickness. The contrast in these images depicts anatomical details of the brain by numerous dark lines of various sizes. These lines are absent in the image taken by the usual spin echo sequence. They represent the blood vessels in the image slice and appear when the deoxyhemoglobin content in the red cells increases. This contrast is most pronounced in an anoxy brain but not present in a brain with diamagnetic oxy or carbon monoxide hemoglobin. The local field induced by the magnetic susceptibility change in the blood due to the paramagnetic deoxyhemoglobin causes the intra voxel dephasing of the water signals of the blood and the surrounding tissue. This oxygenation-dependent contrast is appreciable in high field images with high spatial resolution.

INTRODUCTION

Magnetic resonance imaging of tissue water in brain provides anatomical details of high image quality which are capable of distinguishing a variety of pathological conditions. This high image quality is achieved only in water proton images. Water is the most abundant compound in most biological tissues and the proton is the nucleus with the highest NMR sensitivity. On the other hand, the water proton concentration, around 75 *M* in tissue, is so high that the resonance signal is insensitive to normal metabolic reactions which involve reactants at concentrations of a few m*M*. Therefore, direct reflection of physiological events in water images has not been observed. If proton MRI from water is to be used for physiological studies of brain, then some indirect effects of physiology must occur. Regional blood flow measurements (*1*) with water images can be one such example since the metabolic activity of brain tissue is well correlated with the oxygen supply and hence to the blood flow.

In this article some new observations of oxygenation level-sensitive contrast in water images are presented as another example of such indirect reflection of physiology. Using high field instruments, we obtained very high spatial resolution brain images with high contrast which are capable of detecting blood vessels as small as 50 to 100 μm in diameter. Such images may provide a means to monitor regional brain activity

* From Department of Biochemistry, Florida State University, Tallahassee, FL 32306 and on AT&T Bell Laboratories Summer Research program (1988).

0740-3194/90 $3.00

in situ in a similar way as positron emission tomography (*2*) is used to map regional oxygen consumption rates in the brain. With a similar objective oxygen level mapping by ^{19}F magnetic resonance imaging of a blood substitute in cat brain has been reported (*3*).

MATERIALS AND METHODS

High resolution images of rodent brains were measured both with a microimaging apparatus attached to a Bruker 360 MHz wide bore spectrometer with a vertical bore magnet and with a 300 MHz imaging spectrometer with a 183-mm horizontal bore magnet (Spectroscopy Imaging Systems Inc.). The field gradients used were up to 4 to 5 G/cm and the slice thickness was 700 μm. The pixel size in the slice plane was 65×65 μm in the data acquisition. In order to get the sensitivity of the probe as high as possible, 15 to 20-mm-diameter saddle coils and surface coils were used. The width of the water peak was 20 to 30 Hz after shimming on a 5-mm-thick slice.

A/J mice (Jackson Laboratory, Bar Harbor, ME) and Sprague–Dawley rats (local commercial source) were anesthetized with interperitoneal injections of pentobarbital (50 mg/kg) and in most cases with an additional 25 mg/kg of the drug subcutaneously. With the vertical magnet (360 MHz), a mouse or a rat (85 to 100 g) held in a vessel was placed upside down in the probe. The heart rate of the animal was monitored by attaching wire electrodes near the chest. A typical heart rate of an anesthetized mouse was 300 to 340 beats/min. When the animal was placed in the probe and breathing 100% oxygen, the rate was near 300 beats/min and when breathing air it was around 250 beats/min. Although the mouse was breathing without assistance, the oxygen uptake in the lungs seemed to be rather inefficient under this anesthetic condition. When the mouse was breathing air, the image of the carotid arteries had much lower signal intensities than the image of the mouse breathing 100% oxygen. This indicated a low oxygenation level of the blood as one would expect from the loss of redness in skin color observed in the mouse breathing air. Although we did not measure the oxygenation level of the circulating blood in these animals, the anesthetizing condition, dependent on such factors as the type of drug and its dosage, seemed to have a strong influence on the oxygenation level in these murine animals. The signal acquisition was not synchronized to the heart beat.

RESULTS

The effect of the blood oxygenation on the mouse brain image is shown in Fig. 1. The images, coronal slices of a mouse head, were obtained with a simple gradient echo pulse sequence. The main magnetic field was normal to these slice image planes. When the mouse, anesthetized with pentobarbital, was breathing 100% oxygen with a heart rate of 280 beats/min, the image (Fig. 1a) showed some features of the brain tissue organization but the contrast was quite poor. However, dramatic changes in the brain image (Fig. 1b) were observed when the oxygen content in the breathing gas was reduced to 20% (the heart rate was 235 beats/min). This change in the contrast was completely reversible. Many dark lines appeared in the image. The prominent ones were along the boundaries of the organizational elements of the brain. Optical microscopy of fixed slices prepared from an excised brain showed many blood

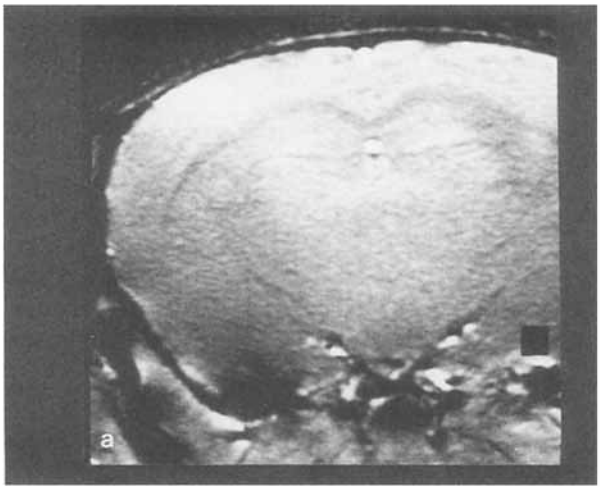
a

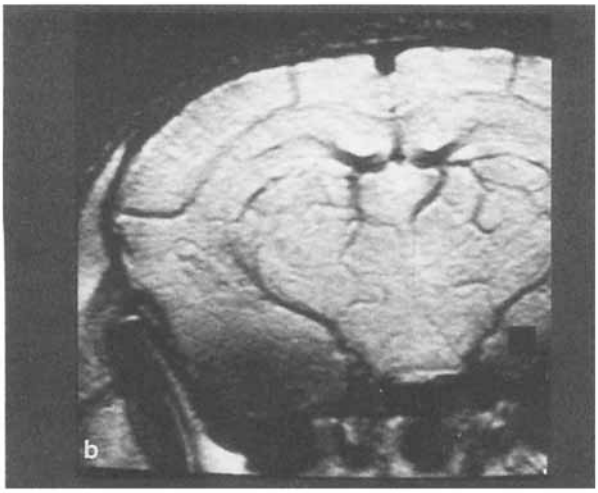
b

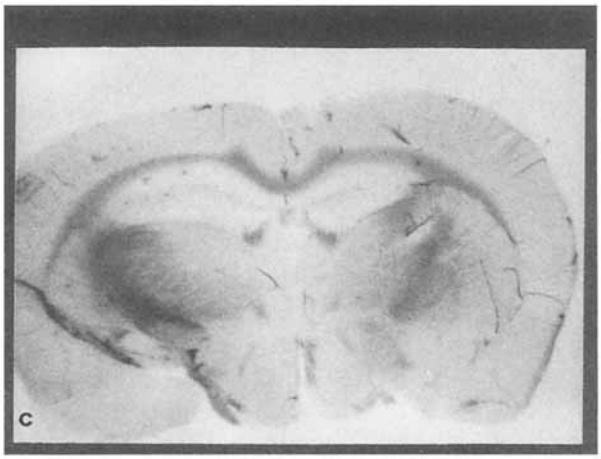
c

vessels in these boundaries. In the region of the cerebral cortex, numerous small blood vessels were seen in the photograph of a fixed slice (Fig. 1c). Correspondingly in these coronal slice images (Fig. 1b and also Fig. 3a described later) there were many narrow dark lines running perpendicular to the arachnoid surface in the cerebral cortex. When the content of oxygen in the breathing gas was incrementally changed from 50 to 20% in experiments at 360 MHz, the contrast of these images changed gradually. Similar images of rat and mouse brains were also obtained with the 7 T horizontal bore magnet where these animals were placed in their natural position relative to the gravitational field.

The contrast of these images was dependent on the length of the echo time in the image acquisition sequence, especially when the oxygen supply was low. With a longer echo time, the widths of some dark lines and the size of dark regions became enlarged. This indicated that there was a distribution of the signal decay time around these dark regions. In Fig. 2, plots of signal intensities at various locations in such images as shown in Figs. 1a and 1b vs the echo time are shown. Two of these locations in the images were in the hippocampal region (*4*), one was on the dark line (between CA1 and CA3) and the other was in the light part (CA1). A spot in the cerebral cortex was on one of the dark lines. The signal decay rates (the slopes of the plots) were strongly dependent on the oxygenation in the dark regions seen in Fig. 1b and the signal from cerebral spinal fluid, as identified by a long T_2 value, was insensitive to the blood oxygenation.

As a further test for determining the cause of the contrast enhancement, an anesthetized mouse was sacrificed by keeping it in a carbon monoxide atmosphere until the color of the lips turned pink and its heart stopped. Most of the contrast seen in Fig. 1b disappeared from the image of the brain. On the other hand, when a mouse was left under an anoxic condition, the image contrast (Fig. 3a) was very high. In this case the flow of the blood was absent and the level of blood oxygenation was presumably very low as the purple color of the lips indicated. These observations strongly indicate that the image contrast was caused by the magnetic susceptibility difference between the blood with paramagnetic deoxyhemoglobin and the surrounding tissues. With diamagnetic oxy or carbon monoxy hemoglobin, the contrast was absent.

There was a striking difference in the image contrast between the gradient echo image (Fig. 3a) and the spin echo image (Fig. 3b) both with a 10 ms echo time at the same slice location in the brain of a dead mouse. The dark lines seen in the gradient echo image (Fig. 3a) were mostly absent in the spin echo image and only faint lines were recognizable at their corresponding locations. Since the process of "time reversal" by the 180° pulse in the spin echo sequence prevented the signal decay during

---

FIG. 1. Coronal slice images of a mouse brain at 360 MHz (a, b). These were gradient echo images and the slice plane was perpendicular to the B_0 field. The pixel size and the slice thickness were 65 × 65 and 700 μm at the data acquisition. The black square in the image is 500 × 500 μm in size. These images were acquired with a 6 ms echo time and a repetition time of 1 s with 256 phase encoding steps. The signals were accumulated four times. (a) Breathing 100% oxygen with the heart rate of 280 beats/min. (b) Breathing air with the heart rate of 235 beats/min. (c) A fixed slice (300 μm thick) of an exercised mouse brain. Most of the dark lines corresponded to blood vessels except those fibrous structures in the region of the thalamus nucleus.

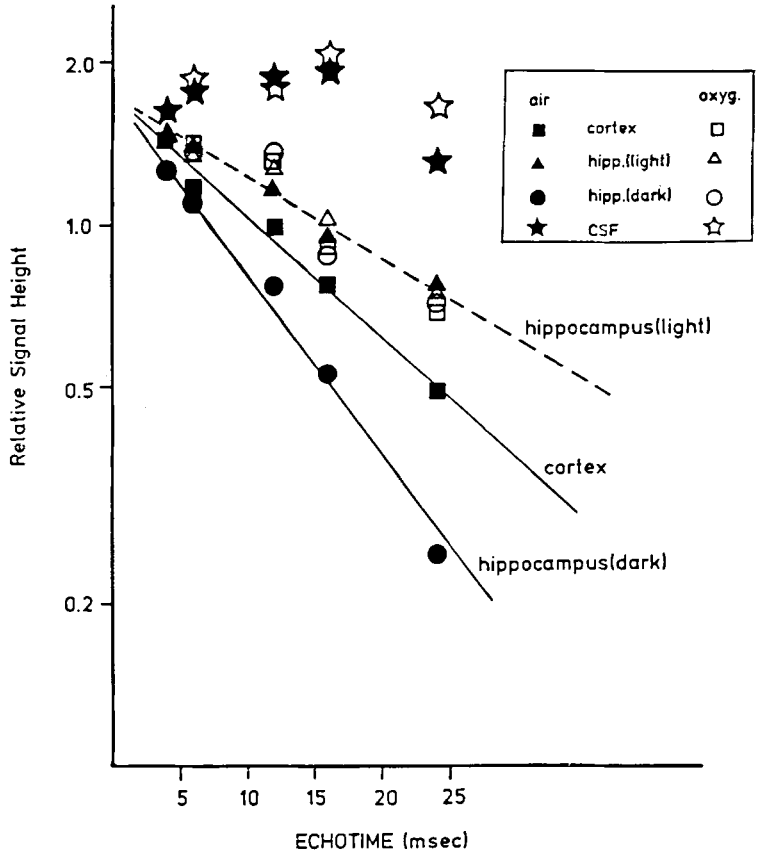

FIG. 2. Signal decays as a function of echo time in gradient echo images of a mouse brain. The open and the closed symbols are used for the image signals of a mouse breathing 100% oxygen and 20% oxygen, respectively. Various symbols are for those spots selected at a dark region between CA1 and CA3 (○) and a light region in CA1 (△) of the hippocampal region (4). Other symbols in this figure are from a dark line in the cerebral cortex (□) and at a region with cerebral spinal fluid (☆) in such slice images as the one shown in Fig. 1b.

the echo time, the cause of the contrast could not be a dynamic phenomenon such as blood flow or water diffusion (the shortening of T_2 of blood water due to the red cells with deoxyhemoglobin) (*5*), but a static phenomenon such as chemical-shift difference or field inhomogeneity. Furthermore, the signal that decayed quickly and gave these dark lines in the gradient echo image was not all coming from the water in blood vessels. The contribution of the blood water was only a small part of it (see Discussion). Otherwise, the spin echo image would have had the same contrast.

It is well known that upon deoxygenation the magnetic susceptibility of blood changes and the T_2 value of blood water becomes short (*6, 7*). We examined those values at the 360 MHz resonant frequency and tested the images of blood samples. The T_2 value measured by 90–t–180–t–sequence was 4 ms for deoxygenated blood (guinea pig blood, hematocrit 0.35) and was 50 ms for oxygenated blood. The mag-

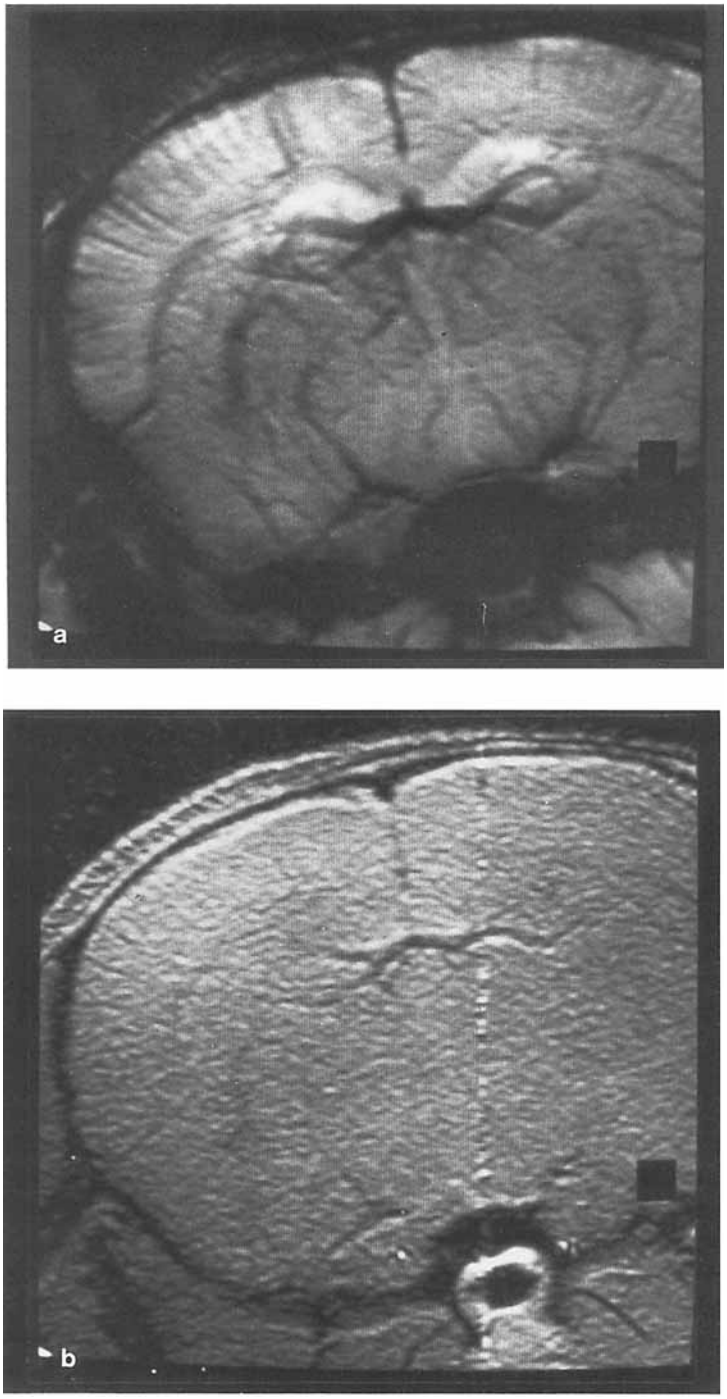

FIG. 3. A comparison of the gradient echo (a) and the spin echo (b) images of an anoxic mouse brain. The coronal slice images were at a different location from those in Fig. 1.

netic susceptibility change was examined in a concentric double tube (blood in the center capillary and saline in the outer tube), the axis of which was placed parallel to the static magnetic field. The shift of the blood water peak relative to the peak of the saline water was essentially zero with oxygenated blood and −150 Hz (down field) with deoxygenated blood. The corresponding volume magnetic susceptibility change was 0.1×10^{-6} as reported by Thulborn *et al.* (*6*). The width of the blood water peak was 250 Hz at the half height.

We obtained several images of a capillary tube (1.4 mm o.d. and 1.0 mm i.d.) filled with blood and placed in a saline bath in order to examine the susceptibility effect in the blood vessel images. To avoid red cell sedimentation during the experiment, heparinized blood from a rat was spun down to have a hematocrit of 65% prior to being filled into the tube. The tube was placed perpendicular to the main field and the slice plane was chosen to be perpendicular to the tube axis. With oxygenated blood in the tube, the spin echo image and the gradient echo image (Figs. 4a and 4b) of the cross section of the tube were quite similar to each other, showing a proper size and shape. The effect of the thin glass wall was minimal. When the tube was filled with deoxygenated blood, the two types of images (Figs. 4c and 4d) became quite different from each other and also from those with oxygenated blood. The signal of the blood water was very weak because of the much shorter T_2 compared with the echo time of the image acquisition, and it should appear black in the images. In the spin echo image, there was a shape distortion due to the shift of the resonance frequency of the nearby water in the saline bath. In the gradient echo image, the dark area extended far beyond the cross-sectional area of the tube. When the slice plane was parallel to the tube axis but the tube orientation relative to the main field was kept the same, the gradient echo image had a much wider dark area in the radial direction of the tube than the spin echo image, which had a width close to the normal size. When the capillary tube with deoxygenated blood was placed parallel to the main field, the spin echo and the gradient echo images did not show any difference in their shapes and displayed the proper size. The signal of the blood water was too weak to be observable, leaving a void space (black area) in the image. Figure 4e shows the gradient echo image of a slice whose plane was perpendicular to the tube axis and therefore also to the main field. The displayed image size is smaller by a factor of 2 than the other images in Fig. 4. There were air bubbles on the side of the bath wall and they had dark halo circles around their images, the origin of which was also the susceptibility effect.

DISCUSSION

The high resolution *in vivo* brain images of a mouse or rat (Fig. 1b and Fig. 3a) show the anatomical details of the brain organization and closely resemble histological slice pictures published in the rat brain atlas (*4*). In the image, the boundaries of various elements of the brain are depicted by dark lines which enhance the contrast. At these boundaries (ventricles and fissures) there are many large blood vessels observable in excised brain slices under an optical microscope. Numerous small blood vessels running perpendicular to the arachnoid surface in the cerebral cortex (Fig. 1c) are also seen. One can find many narrow dark lines with a similar geometry in

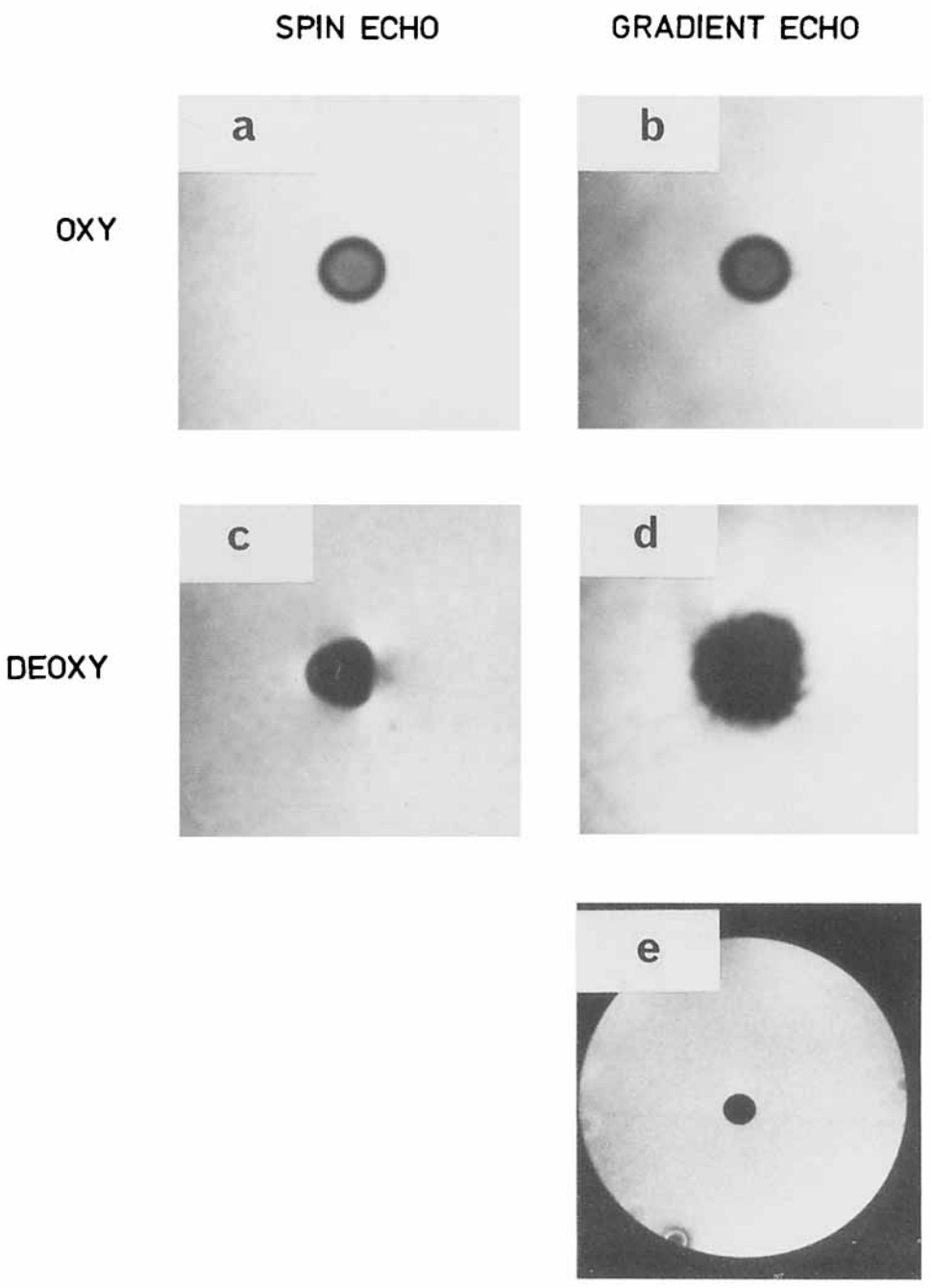

FIG. 4. The spin echo and gradient echo images of a capillary tube with blood in a saline bath. (a–d) The tube axis was perpendicular to the main field and to the slice plane. The tube (1.4 mm o.d. and 1 mm i.d.) was filled with either oxygenated or deoxygenated blood (hematocrit 65%). The spatial resolution of these images was 133 × 133 μm in pixel size. The echo time was 10 ms for a and b and 24 ms for c and d. (e) The tube axis was parallel to the main field and perpendicular to the slice plane. A tube of the same size was filled with deoxygenated blood. The spatial resolution was 66 × 66 μm in pixel size. The echo time was 10 ms. This gradient echo image was displayed to show the size of the tube to be a factor of 2 smaller than the other images.

the MR images (Figs. 1b and 3a). The appearance of these dark lines was dependent on the blood oxygenation level and they disappeared when the blood was completely oxygenated (Fig. 1). The presence of paramagnetic deoxyhemoglobin (the high spin ferrous state) in blood was responsible for the appearance of dark lines, while diamagnetic oxy or CO hemoglobin (the zero spin ferrous state) did not give the contrast. The contrast was observed in gradient echo images but not in spin echo images. From these observations, the cause of the contrast was thought to be the magnetic susceptibility change in blood relative to the surrounding tissues.

It is well known that the field homogeneity is degraded at the boundary of two materials which have different magnetic susceptibilities. Due to the susceptibility difference, the boundary can appear with higher contrast in a gradient echo image (*8, 9*) than in a spin echo image. In deoxygenated blood, large field inhomogeneities are generated inside and around red cells (*5*). These field inhomogeneities or field gradients within the diffusion distance of water molecules are responsible for the shortening of the blood water T_2. In addition to this, the averaged magnetic susceptibility of deoxygenated blood is still significantly different from the susceptibility of surrounding tissues and therefore the field variation can also extend beyond the boundary of a blood vessel.

When a blood vessel is running parallel to the main magnetic field, there is no field variation around the vessel as shown in the *in vitro* experiment with a blood sample described earlier (Fig. 4e). In the coronal slice images of Fig. 1 (normal to the main field), one can see the cross sections of the blood vessels, various arteries at the base of the brain, and the sagical sinus at the top of the brain where venus blood flows. When a blood vessel which contains paramagnetic deoxyhemoglobin is normal to the main magnetic field, there is a region with a varying magnetic field around it. The variation of the field (ω_s) near a blood vessel (a long cylinder with an inner radius a) at the distance of r from the its center ($r \geq a$) can be expressed by

$$\omega_s/\omega_0 = 2\pi\Delta\chi\left(\frac{a}{r}\right)^2(2\cos^2\theta - 1). \qquad [1]$$

In Eq. [1] $\Delta\chi$ is the difference of the volume magnetic susceptibilities of the blood and the surrounding tissue and θ is the angle which the radial vector **r** makes with the main field and ω_0 is the resonance frequency of the tissue water far away from the blood vessel (*10–13*). The value of $\Delta\chi$ is proportional to the degree of deoxygenation of the blood. Taking the degree of the deoxygenation to be 50% and $\Delta\chi$ to be 0.05×10^{-6}, the variation in ω_s/ω_0 is estimated to be ± 0.08 ppm at a distance of $r = 2a$. With this field variation, the echo signal develops a phase difference of $\omega_s \cdot t_e$ during the echo time (t_e) relative to the echo signal without the extra field. The tissue water signal $S(x', y')$ at a pixel (x', y') in the slice image can be expressed in the following way after taking the two dimensional Fourier transform where the T_2 decay term is neglected:

$$S(x', y') = A\left|\int_{\text{voxel}} dv \exp(i\omega_s \cdot t_e)\delta(\omega_x + \omega_s - \omega_{x'})\right|. \qquad [2]$$

In Eq. [2], ω_x and $\omega_{x'}$, are the angular frequencies at x and x' along the read gradient

axis in the object space and in the image space, respectively, and δ is a delta function which has a value of 1 for the signal at x when $\omega_x + \omega_s$ falls within the frequency range of the voxel centered at $\omega_{x'}$ and has a value of zero otherwise. When ω_s is larger than the pixel size in frequency, the signal is shifted along the read gradient axis to a nearby voxel. The volume integral in Eq. [2] is over the voxel of $\omega_{x'}$, counting all the signals in the voxel. This includes those shifted into it from various positions of x. The summing should be a vectorial addition with the phase term $\exp(i\omega_s \cdot t_e)$. In spin echo image acquisition, the phase inversion by the 180° pulse makes the dephasing factor zero provided that the 180° pulse is at the center of the total echo time period in the sequence. All the signals in the voxel are then in phase, but the above-mentioned chemical-shift artifact induced by the shift ω_s appears in the image (Fig. 4c). In the gradient echo acquisition the vectorial summation in the voxel causes some signal cancellation (intra-voxel dephasing effect) and the tissue water image shows dark regions around the vessel cylinder in addition to the chemical-shift artifact (Fig. 4d).

We have made calculations of the above dephasing effect to simulate the images obtained from the blood samples mentioned earlier (*14*). The point to be made here is that the region which contributes the intra-voxel dephasing extends as far as two times the vessel diameter, and in some case greater, as judged by the dark area in the calculated image. This means that the volume which contributes to the dephasing is four times that vessel volume if one treats a cylinder as a two-dimensional object. The direction of the slice gradient, if it is not parallel to the cylinder axis, is one linear dimension of the two. This could be the reason why the dark lines representing the blood vessels in the slice plane were observable despite the slice thickness of several hundred microns (Figs. 1 and 3). In the other linear dimension, normal to the cylinder axis in the slice plane, the width of the dark lines could be twice as large as the actual blood vessel sizes. In other words, the dark lines in the gradient echo image were exaggerated. In the comparison of the spin echo image with the gradient echo image in Fig. 3, the lines seen in the spin echo image are much narrower and less distinct than those in the gradient echo image. This exaggeration or contrast enhancement is dependent on the value of ω_s and therefore ω_0. At a lower field strength the contrast would be hard to observe and at much higher fields the contrast becomes overly exaggerated or the image distortion may become unacceptable. We have tested two frequencies (360 and 300 MHz) so far.

Although the contrast described above is sensitive to the blood oxygenation, it is difficult to estimate the degree of the oxygenation from the extent of the contrast. The intra-voxel dephasing or the apparent signal decay rate, such as the one shown in Fig. 2, would depend not only on the oxygenation level but also on the size and geometry of the blood vessels in the magnetic field. When blood vessels are parallel to the main field, the blood oxygenation level could be estimated from the relaxation time T_2 of the blood water, since it is strongly dependent on the degree of oxygenation (*15*). These subjects need further study.

In conclusion, gradient echo images of the brain at high fields give a high image contrast which is sensitive to the blood oxygenation level. Although we have not shown the distinction between arterial blood vessels and venus blood vessels at various locations in the brain, we expect this oxygenation-sensitive contrast could be used to monitor regional oxygen usages in the brain. When some region in a brain is much

more active than other regions, the active region could show darker lines in the image because of the increased level of deoxyhemoglobin resulting from higher oxygen consumption. The oxygen usage in the brain is supposed to be tightly coupled to the metabolic activity of the brain cells (*16*). Therefore, in addition to the anatomy of the brain, one aspect of its physiology can be studied by the MRI of water.

REFERENCES

1. C. L. DUMOULIN, S. P. SOUZA, AND H. R. HART, *Magn. Res. Med.* **5,** 238 (1987).
2. M. E. RAICHLE, M. A. MINTUM, AND P. HERSCOVITCH, *in* "Brain Imaging and Brain Function" (L. Sokoloff, Ed.), pp. 51–59, Raven Press, New York, 1985.
3. D. EIDELBERG, G. JOHNSON, D. BARNES, P. S. TOFTS, D. DELPY, D. PLUMMER, AND W. I. MCDONALD, *Magn. Res. Med.* **6,** 244 (1988).
4. G. PAXINOS AND C. WATSON, *in* "The Rat Brain," Figure 36, Academic Press, Orlando, 1986.
5. K. M. BRINDLE, F. F. BROWN, I. D. CAMPBELL, C. GRATHWOHE, AND P. W. KUCHEL, *Biochem. J.* **180,** 37 (1979).
6. K. R. THULBORN, J. C. WATERTON, P. M. MATHEWS, AND G. K. RADDA, *Biochim. Biophy. Acta* **714,** 265 (1982).
7. R. A. BROOKS AND G. DI CHIRO, *Med. Phys.* **14,** 903 (1987).
8. I. J. COX, G. M. BYDDER, D. G. GADIAN, I. R. YOUNG, E. PROCTOR, S. R. WILLIAMS, AND I. HART, *J. Magn. Res.* **70,** 163 (1986).
9. J. FRAHM, K. D. MERBOLDT, AND W. HAENICKE, *Magn. Res. Med.* **6,** 474 (1988).
10. C. A. REILLY, H. M. MCCONNELL, AND R. G. MEISENHEIMER, *Phys. Rev.* **98,** 264A (1955).
11. M. G. MORIN, G. PAULETT, AND M. E. HOBBS, *J. Phys. Chem.* **60,** 1594 (1956).
12. D. C. DOUGLASS AND A. FRATIELLO, *J. Chem. Phys.* **39,** 3161 (1963).
13. J. D. JACKSON, *in* "Classical Electrodynamics," pp. 110–119, Wiley, New York, 1963.
14. S. OGAWA AND T. M. LEE, *Magn. Reson. Med.*, in press.
15. K. R. THULBORN, C. J. WATERTON, AND G. K. RADDA, *J. Magn. Res.* **45,** 188 (1981).
16. B. K. SIESJÖ, *in* "Brain Energy Metabolism" p. 106, Wiley, New York, 1978.